HHS Public Access

Author manuscript

*Nat Neurosci*. Author manuscript; available in PMC 2011 March 01.

Published in final edited form as:

*Nat Neurosci*. 2010 September ; 13(9): 1047–1049. doi:10.1038/nn.2609.

# Regulation of Fast-Spiking Basket Cell Synapses by the Chloride Channel ClC–2

**Csaba Földy**[1,2], **Sang-Hun Lee**[1], **Robert J. Morgan**[1], and **Ivan Soltesz**[1]

[1]Department of Anatomy and Neurobiology, University of California, Irvine

## Abstract

Parvalbumin-expressing, fast-spiking basket cells play key roles in the generation of synchronous, rhythmic population activities in the hippocampus. Here we show that $GABA_A$ receptor-mediated synaptic inputs from murine parvalbumin-expressing basket cells are selectively modulated by the membrane voltage- and intracellular chloride-dependent chloride channel ClC–2. These data demonstrate a novel cell type-specific regulation of intracellular chloride homeostasis in the perisomatic region of hippocampal pyramidal neurons.

### Keywords

interneuron; $GABA_A$ receptor; excitability; microcircuit; intracellular chloride

There are two distinct basket cell classes specialized to provide GABAergic innervation to the perisomatic region of principal cells, the parvalbumin- or cholecystokinin- expressing basket cells (PVBCs or CCKBCs, respectively). The intrinsic and synaptic properties of PVBCs enable them to perform circuit functions related to precise time keeping and generation of network oscillations, whereas CCKBCs are thought to serve as modulators that adapt network activity to behavioral states1,2. Because synapses from PVBCs and CCKBCs co-exist on the perisomatic membrane, it has been assumed that the regulation of the intracellular concentration of $Cl^-$, the major charge carrying anion for $GABA_A$ receptor-channels, is uniform at PVBC and CCKBC synapses. Here we demonstrate using paired recording techniques3 in slices (Supplementary Methods online) that the chloride channel ClC–2 robustly modulates synaptic inputs specifically from PVBCs, providing a molecular safety mechanism for the prevention of the accumulation of intracellular chloride at the highly active GABAergic synapses formed by the fast-spiking PVBCs. Our experimental protocols were approved by the Institutional Animal Care and Use Committee of the University of California, Irvine.



**Correspondence:** Csaba Földy, PhD, Department of Molecular and Cellular Physiology, Stanford University, Palo Alto, CA 94304-5552, foldy@stanford.edu.

**Author contributions:** C.F. designed the experiments. C.F., S.-H.L. and R.J.M. performed the experiments and analyzed the data. C.F. and I.S. wrote the manuscript.

[2]Present address: Department of Molecular and Cellular Physiology, Stanford University, Palo Alto

Paired interneuron-pyramidal cell whole-cell patch clamp recordings showed that, at membrane potentials more depolarized than −35 mV, the amplitudes of the unitary IPSCs evoked by CCKBCs (CCK-IPSCs) were smaller than the PVBC-evoked IPSCs (PV-IPSCs) (Fig. 1a). On the other hand, below the reversal potential for $GABA_A$ receptor-mediated events ($E_{GABAA}$), it was the PV-IPSCs that were significantly smaller than the CCK-IPSCs (Fig. 1a). Furthermore, examination of the current-voltage relationships across a wide voltage range (Fig. 1a) indicated that CCK-IPSCs exhibited inward rectification (inward current flowed more easily than outward current), while PV-IPSCs showed apparent outward rectification.

The origin of the inward rectification of CCK-IPSCs was readily identifiable, as it was due to depolarization-induced suppression of inhibition1 (DSI) that was sensitive to the CB1 receptor antagonist AM251 (10 μM) (Fig. 1a, inset). However, the difference in amplitude of the inward IPSCs was unexpected, because the number of $GABA_A$ receptor-channels is similar at PVBC and CCKBC synapses on CA1 pyramidal cells4. In order to characterize the apparent outward rectification of PV-IPSCs, we compared the inward and outward portions of the current-voltage relationships (ΔIPSC/ΔV, reflecting synaptic conductance; see Supplementary Methods). While the average ΔIPSC/ΔVs of inward and outward CCK-IPSCs were not different (in AM251; 37.7±8.5 and 51.8±14, n=4 pairs, P=0.424), the average ΔIPSC/ΔV for inward PV-IPSCs was significantly smaller than for outward PV-IPSCs (Fig. 1b; 7.6±1.5 and 18±2.9, n=8 pairs, P=0.007, Fig. 1b). Consequently, the ratio of the average ΔIPSC/ΔV of inward versus outward currents (reflecting rectification) was also significantly smaller for the PV-IPSCs (0.43±0.04 vs. 0.75±0.06, n=8 vs. n=4 pairs, P=0.001).

An explanation for the smaller inward PV-IPSCs compared to the CCK-IPSCs is that the driving force for $Cl^-$ is lower at PVBC compared to CCKBC synapses. Indeed, paired recordings with low (4 mM) intracellular $Cl^-$ concentration close to physiological values5 revealed that the difference in inward IPSC amplitude between the PVBC and CCKBC inputs was accompanied by differences between the $E_{GABAA}$ values (PVBC: −70.8±0.9 mV, n=8 pairs; CCKBC: −67.8±0.9 mV, n=13 pairs, P=0.04; Supplementary Fig. $1a_1$), indicating lower intracellular $[Cl^-]_i$ at PVBC synapses. Such differential regulation of $[Cl^-]_i$ could conceivably occur at the level of individual synapses and/or sub-cellular domains5-8. Since synapses from the two types of basket cells intermingle and are assumed to distribute similarly on perisomatic membranes, we performed a morphological analysis of our recorded pre- and postsynaptic cell pairs (Fig. 1c). The results revealed that PVBC axons formed more putative synaptic terminals on the postsynaptic pyramidal cells compared to CCKBCs (11±0.6, n=15 pairs vs. 8.3±0.8, n=14, P=0.02; note, however, that the number of release sites per terminal may differ between PVBCs and CCKBCs; for a review, see Ref. 1). In addition to differences in the total number of terminals, the distribution of the terminals within the perisomatic compartment was also different. Namely, PVBCs formed approximately twice as many axon terminals on the soma (5.8±0.7, n=15 pairs vs. 2.3±0.8, n=14 pairs, P=0.02), while the CCKBC terminals extended farther out onto the apical dendrites (Fig. 1d).

The preferential cell type-dependent innervation of sub-cellular compartments may provide anatomical basis for a hypothetical mechanism conveying domain-specific regulation of $[Cl^-]_i$. Indeed, whole-cell recordings with either low (4 mM) or high (120 mM) intra-pipette $Cl^-$ ($[Cl^-]_{pip}$) from the soma or apical dendrite (60–80 μm from soma, close to the middle of the basket cell synapse distribution in the stratum radiatum, see Fig. 1d) of single CA1 pyramidal cells revealed presence of a hyperpolarization-gated, sustained $Cl^-$-conductance preferentially at the pyramidal cell soma (Fig. 2a; note that these data do not exclude the presence of such a $Cl^-$-conductance elsewhere in the dendritic tree).

Next, paired recording experiments between PVBCs and pyramidal cells were conducted by first evoking large outward PV-IPSCs at +60 mV (and presumably loading the postsynaptic cell body with $Cl^-$; $[Cl^-]_{pip}$=4 mM), and then stepping the membrane potential to −90 mV. Inward PV-IPSCs immediately after the step to −90 mV were large (−37.8±7.5 pA, n=5 pairs), but then the amplitude decreased over tens of seconds (τ=14.4±1.8 sec, n=5 pairs; Fig. 2b), consistent with the presence of a mechanism that lets $Cl^-$ ions exit from the inside to the outside according to the $Cl^-$ electrochemical gradient (note that similar $Cl^-$ extrusion experiments with CCK-IPSCs resulted in a significantly slower decrease in the event amplitude after the step to −90 mV; τ=24.7±3.8 sec, n=5 pairs; P=0.04).

A mechanism that could potentially underlie the above-described effects is the hyperpolarization-activated, inwardly rectifying plasma membrane $Cl^-$-channel ClC–2 whose gating also depends on $[Cl^-]_i$ (a rise in intraneuronal $Cl^-$-concentration opens ClC–2 and results in an efflux of $Cl^-$)9-11. Both mRNA and protein for the ClC–2 channel are known to be expressed in CA1 pyramidal cells, but not in granule cells of the dentate gyrus (GCs)12,13. Consistent with the lack of ClC–2 expression in GCs, paired recordings from PVBCs and postsynaptic GCs revealed no marked outward rectification of the PV-IPSCs, and the somatic $Cl^-$-conductance was also lacking in GCs (Supplementary Fig. 1b). Furthermore, the somatic $Cl^-$-conductance was not present in CA1 pyramidal cells from mice lacking the ClC–2 channel14 (*ClC–2*$^{-/-}$; Fig. 2c). In addition, paired recordings from PVBCs and postsynaptic CA1 pyramidal cells in mice showed increased inward currents (Fig. 2d) and, consequently, significantly reduced outward rectification of PV-IPSCs in *ClC–2*$^{-/-}$ mice (*ClC–2*$^{+/+}$: 0.42±0.05, n=8 pairs and *ClC–2*$^{-/-}$: 0.89±0.06, n=7 pairs, P=0.0005; Fig. 2e). Note that the rectification of the CCK-IPSCs did not change in the *ClC–2*$^{-/-}$ mice (*ClC–2*$^{+/+}$: 0.79±0.08, n=3 pairs and *ClC–2*$^{-/-}$: 0.78±0.05, n=4 pairs, P=0.8; Fig. 2e). Finally, $Cl^-$ extrusion experiments (similar to those in rat in Fig. 2b) showed a significantly slower decrease in the PV-IPSC amplitude after the step to −90 mV in the *ClC–2*$^{-/-}$ (*ClC–2*$^{+/+}$: τ=14.9±1.1 sec, n=4 pairs; *ClC–2*$^{-/-}$: τ=22.6±2.5 sec, n=4 pairs; P=0.03). Additional experiments showed a significantly longer time to reversal of the inward (depolarizing) IPSCs to outward (hyperpolarizing) IPSCs in CA1 pyramidal cells from *ClC–2*$^{-/-}$ mice compared to *ClC–2*$^{+/+}$ after a brief period of intense presynaptic GABAergic fiber activity evoked by multi-fiber extracellular stimulation resulting in increased intracellular $[Cl^-]$ (Supplementary Fig. 1d).

Data in this paper reveal a novel regulation of PVBC synapses by ClC–2. The ClC–2-mediated selective modulation of PVBC inputs appear to be ideally suited to prevent potentially dangerous rises in $[Cl^-]_i$ (and thus depolarizing $GABA_A$ responses) during

episodes of intense synchronized firing during hippocampal network oscillations by populations of fast-spiking PVBCs that form convergent inputs on single pyramidal cells15 (in contrast, CCKBCs fire at lower frequencies in vivo2). Unlike several other $[Cl^-]_i$-regulating mechanisms5, ClC–2 does not influence the resting $[Cl^-]_i$ under normal circumstances when $E_{GABAA}$ is more hyperpolarized than the resting membrane potential. Activation of ClC–2 may also be aided by $K^+$-conductances (e.g., postsynaptic $GABA_B$ receptors) that can hyperpolarize the membrane potential below $E_{GABAA}$, or by extracellular acidification11. Future studies will be required to demonstrate whether differential $[Cl-]_i$ regulation exist even at adjacent synapses from PVBCs and CCKBCs, and whether the differential activity of ClC–2 at PVBC inputs is due to differences in the levels of ClC–2 expression (i.e., ClC–2 may exist at some CCK synapses13) and/or channel modulation11.

## Supplementary Material

Refer to Web version on PubMed Central for supplementary material.

## Acknowledgements

We thank Ms R.Zhu for excellent technical assistance, Mr K.Ding and Ms D.Szabadics for camera lucida reconstructions, Ms M.Case for genotyping, Dr J.E.Melvin for the ClC–2 knockout mouse, and Drs L.Hilgenberg, M.A.Smith, M.Cahalan, M.V.Jones, Z.Nusser and R.L.McDonald for discussions. This work was supported by the US National Institutes of Health grant NS38580 (to I.S.) and the Epilepsy Foundation through the generous support of the Eric W. Lothman Training Fellowship (to S.-H.L.).

## References

1. Freund TF, Katona I. Neuron. 2007; 56:33–42. [PubMed: 17920013]
2. Klausberger T, Somogyi P. Science. 2008; 321(5885):53–7. [PubMed: 18599766]
3. Földy C, Lee SY, Szabadics J, Neu A, Soltesz I. Nat. Neurosci. 2007; 10(9):1128–30. [PubMed: 17676058]
4. Klausberger T, Roberts JD, Somogyi P. J.Neurosci. 2002; 22(7):2513–21. [PubMed: 11923416]
5. Blaesse P, Airaksinen MS, Rivera C, Kaila K. Neuron. 2009; 61:820–838. [PubMed: 19323993]
6. Szabadics J, Varga C, Molnár G, et al. Science. 2006; 311:233–235. [PubMed: 16410524]
7. Duebel J, Haverkamp S, Schleich W, et al. Neuron. 2006; 49(1):81–94. [PubMed: 16387641]
8. Inglefield JR, Schwartz-Bloom RD. J.Neurosci.Methods. 1997; 75(2):127–35. [PubMed: 9288644]
9. Madison DV, Malenka RC, Nicoll RA. Nature. 1986; 321(6071):695–7. [PubMed: 2423884]
10. Staley KJ. J.Neurophysiol. 1994; 72:273–284. [PubMed: 7965011]
11. Jentsch TJ. Crit.Rev.Biochem.Mol.Biol. 2008; 43:3–36. [PubMed: 18307107]
12. Smith RL, Clayton GH, Wilcox CL, Escudero KW, Staley KJ. J.Neurosci. 1995; 15:4057–4067. [PubMed: 7751965]
13. Sík A, Smith RL, Freund TF. Neuroscience. 2000; 101:51–65. [PubMed: 11068136]
14. Nehrke K, Arreola J, Nguyen HV, et al. J.Biol.Chem. 2002; 277(26):23604–11. [PubMed: 11976342]
15. Bartos M, Vida I, Jonas P. Nat.Rev.Neurosci. 2007; 8(1):45–56. [PubMed: 17180162]

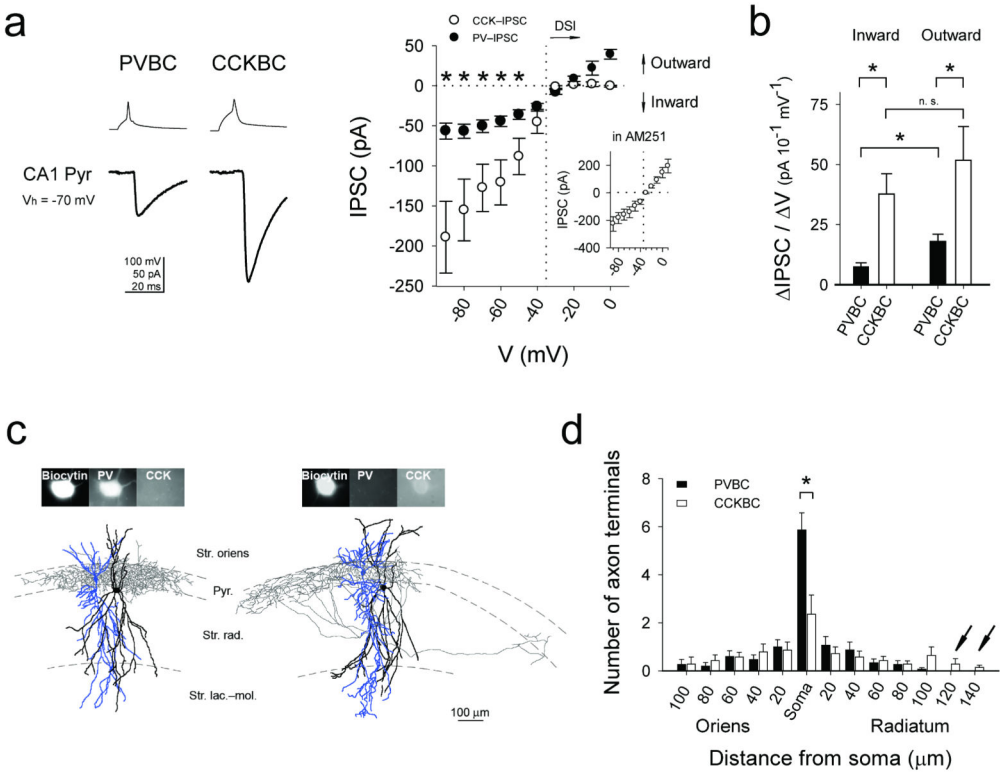


**Figure 1. Outward rectification of PV-IPSCs and distribution of PVBC axon terminals on the somata of pyramidal cells**

**(a)** Left: Averaged example traces; upper: presynaptic spikes; lower: postsynaptic responses ($[Cl^-]_{pip}$=48.7 mM). Right: current-voltage plots of IPSCs (failures included; PVBC: n=6 pairs; CCKBC: n=5 pairs; asterisks indicate P<0.05, errors are s.e.m; probability of release was similar between the two groups, see Supplementary Methods). Inset: CCK-IPSCs in AM251 (n=4 pairs). **(b)** Average ΔIPSC/ΔVs of the plot in (a) (CCK-IPSCs in AM251). **(c)** Examples of basket cells (axons: gray; dendrites: black) and pair-recorded postsynaptic pyramidal cells (blue). **(d)** Distribution of terminals. (P=0.03). Arrows indicate distal CCKBC terminals.

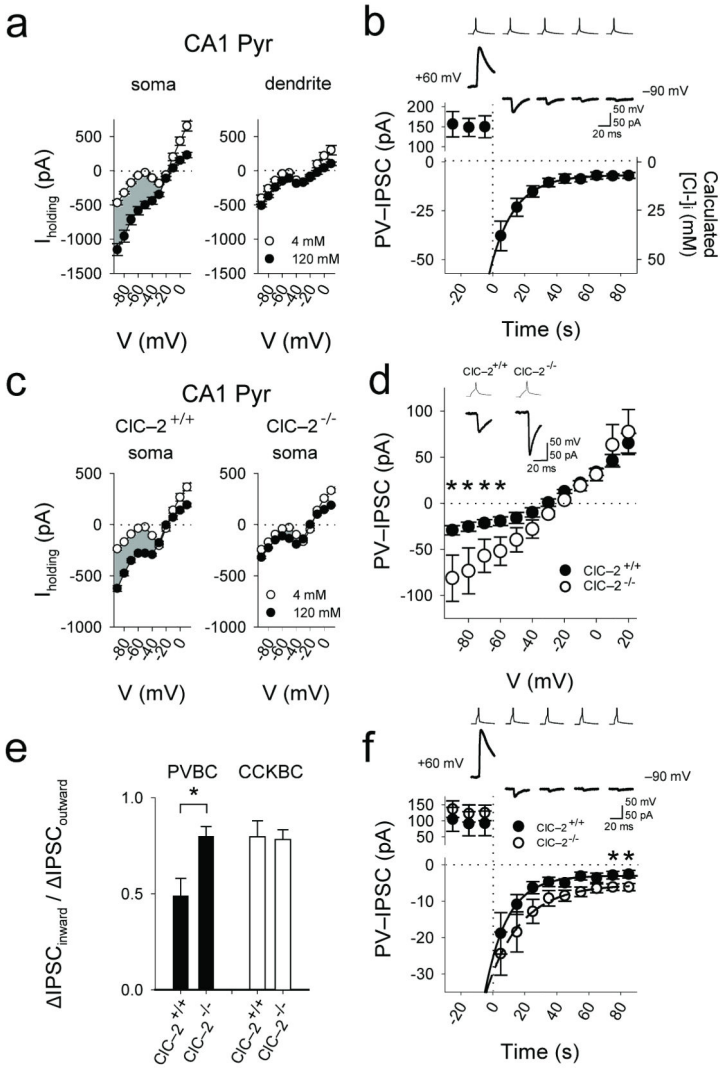


**Figure 2. Somatic hyperpolarization-gated, sustained $Cl^-$-conductance mediated by ClC–2**

**(a)** Whole-cell recordings from the somata and proximal apical dendrites of pyramidal cells with different $[Cl^-]_{pip}$ (4mM: $n_{soma}$=14, $n_{dendrite}$=4; 120mM: $n_{soma}$=11, $n_{dendrite}$=4; shading indicates the difference current reflecting whole-cell $Cl^-$ current). **(b)** Time-dependent decrease of PV-IPSCs after stepping the membrane voltage of the postsynaptic cell from +60 mV to −90 mV in rat. **(c)** Large sustained somatic $Cl^-$-conductance in somata of CA1 pyramidal cells in the wild-type (*ClC–2*$^{+/+}$) but not the *ClC–2*$^{-/-}$ mice (4mM: $n_{soma,+/+}$ =13, $n_{soma,-/-}$ =20; 120mM: $n_{soma,+/+}$ =24, $n_{soma,-/-}$ =24). **(d)** Current-voltage plots of PV-IPSCs from *ClC–2*$^{+/+}$ (n=6 pairs) and *ClC–2*$^{-/-}$ (n=3 pairs). Inset: PV-IPSCs from *ClC–2*$^{-/-}$ mice compared to *ClC–2*$^{+/+}$ (example traces at −70 mV; $[Cl^-]_{pip}$=40 mM). **(e)** Significantly decreased outward rectification of the PV-IPSCs in the *ClC–2*$^{-/-}$ mice, and lack of change in rectification in the case of CCK-IPSCs. **(f)** Slower time-dependent decrease of PV-IPSCs after stepping the membrane voltage of the postsynaptic cell from +60 mV to −90 mV in the *ClC–2*$^{-/-}$ mice compared to *ClC–2*$^{+/+}$. Asterisks indicate significant difference (note that the larger IPSCs indicated by asterisks in these $Cl^-$ extrusion experiments are in general

agreement with the presence of larger IPSCs at hyperpolarized holding potentials in the *ClC–2*$^{-/-}$ animals in Fig. 2d).